BIOCHEMISTRY
including biophysical chemistry & molecular biology

Article

pubs.acs.org/biochemistry

Active Site Binding and Catalytic Role of Bicarbonate in 1,4-Dihydroxy-2-naphthoyl Coenzyme A Synthases from Vitamin K Biosynthetic Pathways

Yueru Sun,[†] Haigang Song,[†] Jie Li,[‡] Ming Jiang,[†,§] Yan Li,[‡,∥] Jiahai Zhou,*[,‡] and Zhihong Guo*[,†]

[†]Department of Chemistry and State Key Laboratory of Molecular Neuroscience, The Hong Kong University of Science and Technology, Clear Water Bay, Kowloon, Hong Kong SAR, China

[‡]State Key Laboratory of Bio-organic and Natural Products Chemistry, Shanghai Institute of Organic Chemistry, Chinese Academy of Sciences, 345 Lingling Road, Shanghai 200032, China

ABSTRACT: 1,4-Dihydroxy-2-naphthoyl coenzyme A (DHNA-CoA) synthase, or MenB, catalyzes a carbon−carbon bond formation reaction in the biosynthesis of both vitamin K1 and K2. Bicarbonate is crucial to the activity of a large subset of its orthologues but lacks a clearly defined structural and mechanistic role. Here we determine the crystal structure of the holoenzymes from *Escherichia coli* at 2.30 Å and *Synechocystis* sp. PCC6803 at 2.04 Å, in which the bicarbonate cofactor is bound to the enzyme active site at a position equivalent to that of the side chain carboxylate of an aspartate residue conserved among bicarbonate-insensitive DHNA-CoA synthases. Binding of the planar anion involves both nonspecific electrostatic attraction and specific hydrogen bonding and hydrophobic interactions. In the absence of bicarbonate, the anion binding site is occupied by a chloride ion or nitrate, an inhibitor directly competing with bicarbonate. These results provide a solid structural basis for the bicarbonate dependence of the enzymatic activity of type I DHNA-CoA synthases. The unique location of the bicarbonate ion in relation to the expected position of the substrate α-proton in the enzyme's active site suggests a critical catalytic role for the anionic cofactor as a catalytic base in enolate formation.

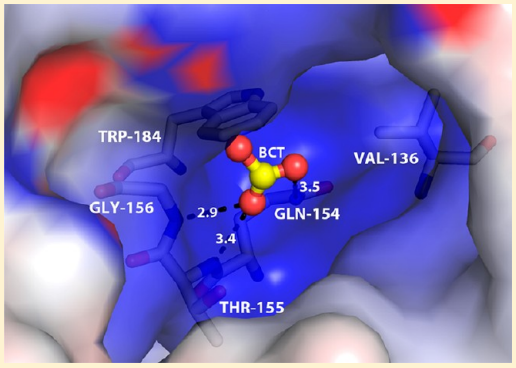

Vitamin K is lipid-soluble naphthoquinone known as menaquinone (K2) in most Gram-positive and Gram-negative facultative bacteria[1] and as phylloquinone (K1) in cyanobacteria, algae, and plants.[2] It is composed of a 1,4-dihydroxynaphthenoid core and a polyprenyl side chain with a varied number of repeating units and serves as an electron transporter either in the bacterial respiratory chain[1] or in photosynthesis.[3] Its biosynthesis from chorismate has been intensively studied in several strains of bacteria[1] and was modified by the recent finding of a new intermediate.[4−6] In humans, vitamin K is not synthesized but is acquired from dietary sources or intestine microflora to serve as a coenzyme in posttranslational γ-carboxylation of glutamate residues.[7] Because of the absence of vitamin biosynthesis in mammals, bacterial enzymes in the menaquinone biosynthetic pathway have become attractive targets for the development of new antibacterial agents.[8−13]

1,4-Dihydroxy-2-naphthoyl-CoA (DHNA-CoA) synthase, also named MenB (EC 4.1.3.36), is an essential enzyme in vitamin K biosynthesis,[14−19] which is responsible for conversion of *o*-succinylbenzoyl-CoA (OSB-CoA) to DHNA-CoA via catalysis of a multiple-step intramolecular Claisen condensation reaction (Figure 1). There are two types of DHNA-CoA synthases with a distinctive bicarbonate dependence of their catalytic activity. The first type (type I) of enzyme is dependent on exogenous bicarbonate for catalytic activity, as found for the orthologues from *Escherichia coli*, *Staphylococcus aureus*, *Bacillus subtilis*, and *Synechocystis* sp. PCC6803.[20,21] The second type (type II) of enzyme, including those from *Mycobacterium tuberculosis* and *Mycobacterium smegmatis*, is intrinsically active but does not respond to externally added bicarbonate.[20] A defining feature of the type I DHNA-CoA synthases is a conserved glycine equivalent to Gly-156 of *E. coli* MenB (*ec*MenB), while a conserved aspartic acid residue occupies this position in the type II enzymes.[20]

The catalytic role of the exogenous bicarbonate in type I enzymes or the equivalent aspartic acid residue in type II enzymes, however, is controversial. Considering that the equivalent acidic groups occupy a position similar to that of the conserved acidic residue responsible for abstraction of a proton from the α-carbon of the coenzyme A thioester substrates in enoyl-CoA hydratases (crotonases) and enoyl-CoA isomerases,[22−28] we proposed that either the exogenous bicarbonate or the conserved aspartate side chain serves as a catalytic base to abstract the succinyl α-proton of the OSB-CoA substrate in the initiation of the intramolecular Claisen condensation.[20] On the other hand, Tonge and co-workers have proposed that the catalytic base is the carboxylate group

Received: April 15, 2012
Revised: May 15, 2012
Published: May 18, 2012

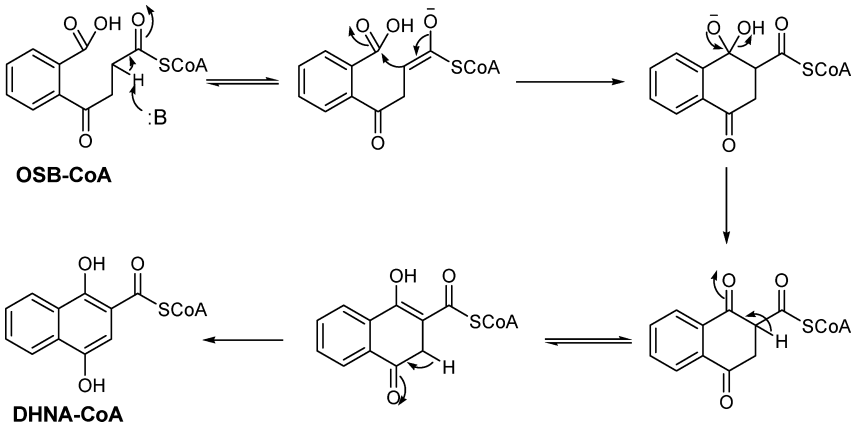

Figure 1. Proposed reaction mechanism of the intramolecular Claisen condensation catalyzed by DHNA-CoA synthase in vitamin K biosynthesis. OSB-CoA, *o*-succinylbenzoyl coenzyme A; DHNA-CoA, 1,4-dihydroxy-2-naphthoyl coenzyme A.

on the benzene ring of the OSB-CoA substrate in either the bicarbonate-insensitive MenB from *M. tuberculosis*[29] or the bicarbonate-sensitive MenB from *E. coli*.[30] In this latter proposal, the substrate carboxylate abstracts the pro-*S* α-proton from the thioester substrate, in contrast to the experimental finding that the pro-*R* α-proton of the OSB-CoA substrate is abstracted.[31] In addition, this proposal offers no explanation for the detected dependence of *ec*MenB activity on bicarbonate.

The proposed role of the exogenous bicarbonate as a catalytic base in type I DHNA-CoA synthases is based on the finding of a bound bicarbonate ion in the crystal structure of MenB from *Salmonella typhimurium* [*st*MenB, Protein Data Bank (PDB) entry 3H02],[32] which was surprisingly crystallized without externally added bicarbonate. The source of the bicarbonate ion was presumably atmospheric carbon dioxide, which was solvated in crystallization buffer. However, under similar crystallization conditions, *ec*MenB is 96.8% identical in sequence to *st*MenB and binds a chloride ion instead of bicarbonate at the same position.[30] In addition, no bicarbonate is found in the available crystal structures of other predicted type I DHNA-CoA synthases from *St. aureus* (*sa*MenB, PDB entry 2UZF)[33] and *Geobacillus kaustophilus* (*gk*MenB, PDB entry 2IEX).[34] The absence of bicarbonate in the crystal structure of these type I enzymes raises doubt about the interpretation of electron density in the determination of the *st*MenB structure.

To improve our understanding of the bicarbonate dependence of the catalytic activity of the type I DHNA-CoA synthases, we determined the crystal structures of *ec*MenB and the orthologue from *Synechocystis* sp. PCC6803 (*sc*MenB) both in the presence and in the absence of externally added bicarbonate. In addition, we also determined the crystal structure of *ec*MenB in complex with nitrate, an inhibitor directly competing with bicarbonate.[20] Results from these structural studies provide unequivocal evidence that bicarbonate binds to the active site and plays a critical role in the catalytic mechanism of the type I enzymes.

MATERIALS AND METHODS

Chemicals. The following reagents were purchased from Sigma: $NaHCO_3$, $NaNO_3$, isopropyl β-D-thiogalactopyranoside (IPTG), polyethylene glycol (PEG, average MW of ~3350), (±)-2-methyl-2,4-pentanediol (MPD), buffers, and other salts. The MenB substrate OSB-CoA was prepared in situ from (1*R*,6*R*)-2-succinyl-6-hydroxy-2,4-cyclohexadiene-1-carboxylate (SHCHC) using the enzymes MenC and MenE.[20,21] SHCHC was chemoenzymatically synthesized using EntC,[35] MenD,[4,5] and MenH[6,36] from chorismate, which was isolated from an engineered bacterial strain as described previously.[37]

Protein Preparation and Activity Assay. Recombinant enzyme MenB from *E. coli* (*ec*MenB) and *Synechocystis* sp. PCC6803 (*sc*MenB) containing only the native amino acid sequences but without any tags were expressed and purified as described previously.[20,21] Purified *ec*MenB was stored in 25 mM Tris buffer (pH 8.0) containing 10% glycerol, and *sc*MenB was stored in 20 mM glycine buffer (pH 9.75) with 1% glycerol. Each protein was >95% pure as determined by sodium dodecyl sulfate−polyacrylamide gel electrophoresis. The DHNA-CoA synthase activity of the enzymes was assayed with a previously reported method in 200 mM phosphate buffer (pH 7.0) in the presence of 20 mM HCO_3^-.[20]

Crystallization, Data Collection, and Structure Determination. Crystallization trials were performed at 22 °C using the hanging drop vapor diffusion method and the INDEX Screening Kit (Hampton Research). The crystallization conditions were optimized by the secondary and additive screenings to alter the crystal shape and improve the diffraction quality. Typically, 1 μL of the protein solution was mixed in a 1:1 ratio with the reservoir solution to a final volume of 2 μL and equilibrated against 500 μL of the reservoir solution in a sealed 24-well plate. Rodlike crystals of apo-*ec*MenB, >0.3 mm in the longest dimension, were obtained by mixing the protein solution containing 10 mg/mL purified *ec*MenB, 25 mM Tris buffer (pH 8.0), and 10% glycerol with the reservoir solution containing 300 mM NaCl, 100 mM Tris buffer (pH 7.5), and 20% PEG 3350. Similar crystals of *ec*MenB in complex with bicarbonate or nitrate were obtained by mixing 10 mg/mL purified *ec*MenB, 10 mM $NaHCO_3$ or $NaNO_3$, 25 mM Tris buffer (pH 8.0), and 10% glycerol with the reservoir solution containing 2% Tacsimate (pH 7.0, Hampton Research), 100 mM Tris buffer (pH 7.5), and 20% PEG 3350. Meanwhile, monoclinic crystals of *sc*MenB (up to 0.1 mm × 0.3 mm × 0.2 mm) were obtained within 5 days after a protein solution containing 10 mg/mL *sc*MenB with or without 10 mM $NaHCO_3$ had been mixed with a reservoir solution consisting of 0.15 M ammonium acetate, 0.02 M L-proline, 0.1 M Bis-Tris buffer (pH 6.1), and 45% MPD. The harvested crystals were soaked in a cryoprotectant solution containing 80% reservoir solution and 20% glycerol (for *ec*MenB crystals) or 20%

dx.doi.org/10.1021/bi300486j | *Biochemistry* 2012, 51, 4580−4589

Table 1. Data Collection and Refinement Statistics[a]

	apo-*ec*MenB	*ec*MenB−HCO_3^-	*ec*MenB−NO_3^-	*sc*MenB−HCO_3^-[b]
PDB entry	4ELX	4ELS	4ELW	4EML
		Data Collection		
space group	$P2_12_12_1$	$P2_12_12_1$	$P2_12_12_1$	$C2$
unit cell dimensions				
a, b, c (Å)	76.5, 133.9, 153.9	76.4, 133.9, 153.3	76.5, 133.9, 153.4	244.6, 140.1, 73.5
α, β, γ (deg)	90, 90, 90	90, 90, 90	90, 90, 90	90, 95.6, 90
redundancy	7.4 (6.1)	6.8 (6.7)	5.7 (5.5)	4.0 (4.0)
completeness (%)	99.4 (89.1)	99.6 (99.1)	99.8 (100.0)	98.1 (94.0)
no. of reflections (unique)	81295 (80858)	69950 (69785)	51971 (49133)	155103 (152169)
I/σ_I	16.5 (3.0)	9.02 (2.3)	12.3 (2.1)	14.1 (6.1)
R_{merge}	0.108 (0.513)	0.199 (0.795)	0.135 (0.754)	0.077 (0.245)
		Refinement		
resolution range (Å)	37.3−2.19	42.8−2.30	42.9−2.55	48.6−2.04
no. of atoms	12633	12408	12289	12897
protein	11950	11981	12038	12139
water	644	382	199	655
ligands/ions	39	45	52	103
average B factor (Å^2)	36.9	38.8	50.1	36.7
protein	36.7	38.7	50.2	36.3
water	41.3	41.8	44.7	44.2
ligand	not available	38.0	51.4	28.7
R_{work}/R_{free}	0.1679/0.2275	0.1825/0.2219	0.1792/0.2257	0.1729/0.2023
deviation from ideal values				
bond lengths (Å)	0.007	0.007	0.008	0.007
bond angles (deg)	1.03	1.04	1.06	0.986
Ramachandran statistics[c]	98.1%, 1.9%, 0%	97.9%, 2.1%, 0%	97.8%, 2.2%, 0%	97.2%, 2.8%, 0%

[a]Values for the highest-resolution shell are given in parentheses. [b]Data for *sc*MenB crystals grown in the presence of 5 mM $NaHCO_3$ are given. Data for crystals grown in the absence of $NaHCO_3$ are similar to those of this crystal. [c]Ramachandran statistics indicate the fraction of residues in the most favored, allowed, and disallowed regions of the Ramachandran diagram, respectively.

ethylene glycol (for *sc*MenB crystals) and stored in liquid nitrogen.

X-ray diffraction data were collected at beamline BL17U at the Shanghai Synchrotron Radiation Facility (SSRF) for the crystals of *ec*MenB and *sc*MenB grown in the presence of $NaHCO_3$. Diffraction images were indexed, integrated, and scaled using HKL2000.[38] The diffraction data for *sc*MenB crystals grown in the absence of $NaHCO_3$ were collected at 100 K using a Rigaku RAXIS IV^{++} imaging plate system with a MicroMax-007 copper rotating anode generator, processed using iMOSFLM,[39] and scaled using SCALA in the CCP4 suite.[40]

All the structures were determined by molecular replacement with Phaser[41] using another wild-type *ec*MenB structure (PDB entry 3T89) as the search model. The obtained structural models were extended by several rounds of manual model fitting and rebuilding with *Coot*[42] and refined using PHENIX[43] or REFMAC5.[44] Noncrystallographic symmetry restraints between monomers were applied for the first round of refinement. Restraints for the ligand HCO_3^-, NO_3^-, or other small molecules from the buffer were imposed and optimized using eLBOW[45] during the structure refinement. MolProbity[46] and PROCHECK[47] were used to assess the overall quality of structural models.

Structural Analysis and Sequence Alignment. All structural analysis was performed with *Coot*,[42] and all graphic presentations of structures were generated using PyMol 1.3.[48] The substrate analogue *o*-succinylbenzoyl-aminoCoA (OSB-NCoA) was taken from a reported structure (PDB entry 3T88) and was manually docked into the *ec*MenB and *sc*MenB holoenzymes in this study, also using PyMol 1.3. The surface electrostatic potential was calculated using the online servers PDB2PQR and APBS.[49,50] Multiple-sequence alignment was conducted using ClustalW 2.0.[51]

RESULTS AND DISCUSSION

Structures of *ec*MenB and Its Complexes with Bicarbonate and Nitrate. All the *ec*MenB crystals belong to space group $P2_12_12_1$ with essentially identical cell dimensions. The initial phases were calculated by molecular replacement using a reported *ec*MenB structure[30] (PDB entry 3T89) as the search model, and the structures of apo-*ec*MenB, the *ec*MenB−HCO_3^- complex, and the *ec*MenB−NO_3^- complex were refined at 2.19, 2.30, and 2.55 Å, respectively. The structural models have good overall stereochemistry with all residues in the most favorable or allowed regions of the Ramachandran diagram. The data collection and refinement statistics for these structures are listed in Table 1.

All the *ec*MenB crystals contain one hexamer in a typical crotonase fold in an asymmetric unit (Figure 2A). As found in all available crystallographic structures of MenB proteins from various sources, each subunit of *ec*MenB is composed of an N-terminal spiral core domain and a C-terminal domain consisting of three helices (residues 225−272, including H10−H12, as shown in Figure 2B) that cross the trimer−trimer interface and form part of active site in the opposing subunit. Residues 87−106 are disordered without discernible electron density in any subunit. Except for one subunit (chain E) in the apo-*ec*MenB structure, the other subunits in the crystal structures with or without anionic ligands are essentially identical with a root-

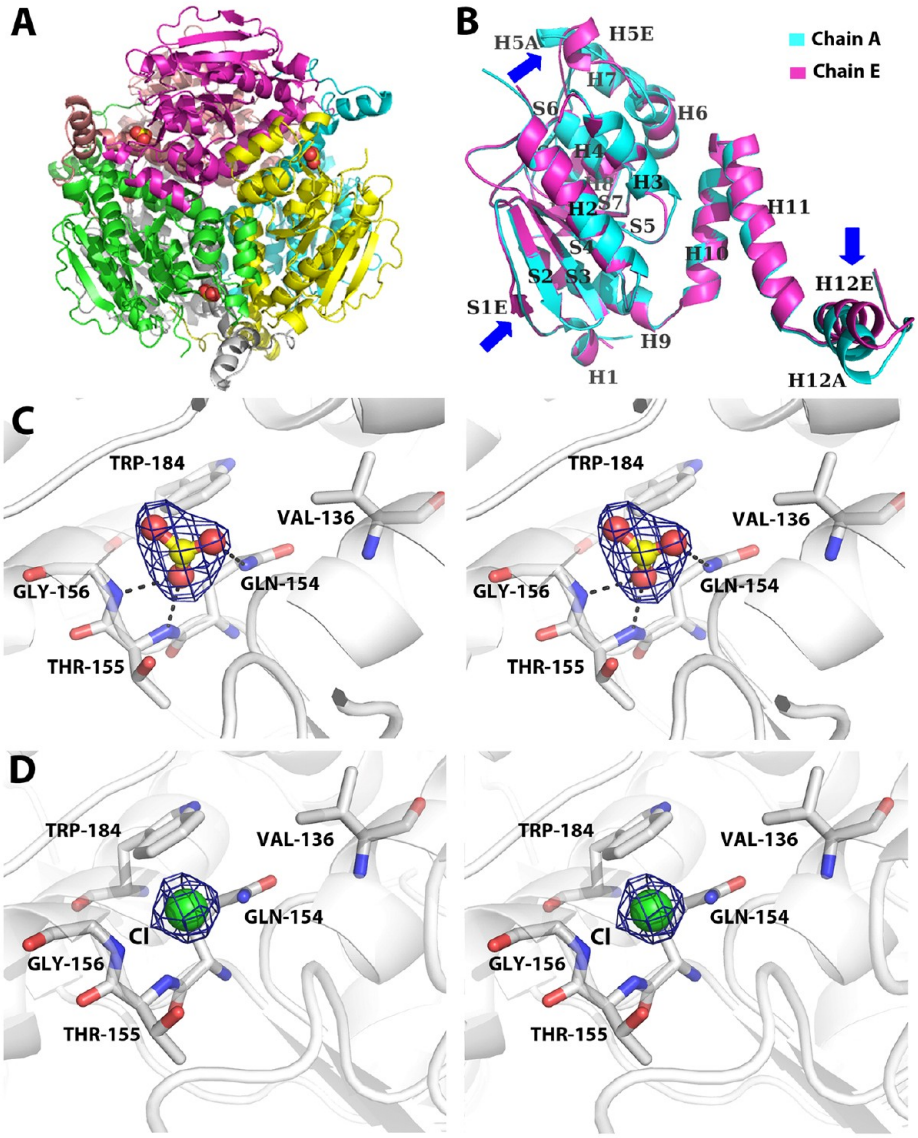

Figure 2. Crystal structures of *ec*MenB in complex with chloride or bicarbonate. (A) Hexameric structure of the *ec*MenB−HCO_3^- complex viewed along the 3-fold axis of the two trimers. The protein is colored by subunit, and the bicarbonate ions are shown as spheres. (B) Superposition of two different monomeric subunits (chains A and E) in the apo-*ec*MenB structure. Three apparent structural differences are indicated by blue block arrows. The α-helices (H) and β-pleated sheets are labeled sequentially from the amino terminus to the carboxy terminus. Secondary structures with A or E in the labels belong to chain A or chain E, respectively. (C) Stereoview of the electron density of bicarbonate in the *ec*MenB−HCO_3^- complex. The anion is represented as sticks with a yellow carbon atom with the surrounding residues shown as sticks. Its $2F_o - F_c$ electron density is contoured at 1.5σ (dark blue mesh). Dashed lines indicate potential hydrogen bonding interactions. (D) Stereoview of the electron density of chloride (green) in apo-*ec*MenB at the anion binding site. The same surrounding amino acid residues are represented as sticks. The $2F_o - F_c$ electron density is contoured at 1.5σ (dark blue mesh).

mean-square deviation (rmsd) of <0.20 Å. As shown in Figure 2B, subunit E of the apo-*ec*MenB structure differs from the other subunits in a 27-residue loop (residues 150−176) connecting S8 and H6, of which a 12-residue fragment, including H5, takes a different spatial arrangement shown by structural superposition. In addition, the orientation of the last C-terminal helix H12 (residues 261−272) is also significantly different from those in the other subunits. Moreover, another difference between chain E of apo-*ec*MenB and the other subunits appears to occur at a three-residue fragment (residues 15−17), which is assigned by PyMol as a short β-pleated sheet in most subunits but as part of the long loop connecting H1 and S2 in chain E (Figure 2B). The structural differences found in the apo-*ec*MenB chain E suggest high flexibility of the MenB structure.

Structure of *sc*MenB. All the *sc*MenB crystals are monoclinic and belong to space group *C*2 with an asymmetric unit containing six monomers, which form two eclipsed trimers. The initial phases were calculated by molecular replacement again using the reported *ec*MenB structure (PDB entry 3T89) as the search model. The structure of *sc*MenB crystals grown in the presence of $NaHCO_3$ was refined at 2.04 Å. All the residues are in the most favorable or allowed regions of the Ramachandran diagram. The data collection and refinement statistics for these structures are listed in Table 1.

The *sc*MenB molecule is also composed of two domains in a typical crotonase fold, of which the C-terminal helices cross the

dx.doi.org/10.1021/bi300486j | *Biochemistry* 2012, 51, 4580−4589

trimer−trimer interface of the hexameric ensemble as found in all other MenB crystal structures. Subunits in these structures can be superimposed with an rmsd of <0.20 Å, and each subunit contains one disordered fragment, residues 78−96, which corresponds to the disordered regions found in all other MenB structures without a bound substrate analogue. The *sc*MenB hexamer can be superimposed with the *ec*MenB hexamers with an rmsd of 0.42 Å over all Cα atoms.

Active Site. The active site of DHNA-CoA synthase has been identified in the crystal structures of its complexes with acetoacetyl-CoA,[29,33] the product,[52] or more recently a substrate analogue.[30] It is located in a deep cleft composed of residues from the N-terminal domain of one subunit and the C-terminal helical domain of the opposing subunit across the trimer−trimer interface. It is composed of a coenzyme A binding site conserved in all the crotonase fold enzymes and a binding site for the acyl portion of the OSB-CoA substrate containing a number of conserved amino acid residues unique to the MenB enzymes.[29,30] The *ec*MenB and *sc*MenB structures contain most of the conserved active site residues interacting with the acyl portion of the substrate with the same position and orientation as in other reported MenB structures. In *ec*MenB structures, these residues form an oxyanion hole consisting of Gly-86 and Gly-133 for stabilization of the enolate intermediate, a hydrophobic patch consisting of Leu-106, Val-108, and Leu-109 for recognition and interaction with the nonpolar aromatic ring of the substrate, and other catalytically essential motifs consisting of Ser-161, Asp-163, and Tyr-258 from a different subunit. In *sc*MenB structures, the corresponding amino acid residues are Gly-77, Gly-123, Leu-96, Val-98, Leu-99, Ser-151, Asp-153, and Tyr-248, respectively. Noticeably, no amino acid residue equivalent to the catalytically essential Asp-185 of *mt*MenB[29] is found in the active site of the structure of either *ec*MenB or *sc*MenB. A glycine residue, Gly-156 in *ec*MenB or Gly-146 in *sc*MenB, occupies the position of the acidic residue in the mycobacterial enzyme in a structural comparison.

*sc*MenB is the first three-dimensional structure of DHNA-CoA synthase in the phylloquinone biosynthetic pathway. It contains 275 amino acid residues and exhibits a high degree of homology with *ec*MenB (66% identical residues). The conservation of the overall structural fold and all the important active site residues in the cyanobacterial enzyme indicates that *sc*MenB is not different in catalytic mechanism from the orthologues in the bacterial menaquinone biosynthetic pathway, consistent with the earlier finding that it possesses the same catalytic activity and bicarbonate dependence as *ec*MenB.[21]

Bicarbonate Binding Site. A bicarbonate anion is present in each subunit of *ec*MenB and *sc*MenB crystals grown in the presence of 5 mM $NaHCO_3$ (Figure 2C). Other small molecules or ions such as water, chloride, glycerol, or MPD from the crystallization buffer do not fit the observed electron density at this position. The simple anion is located on top of Gly-156 of *ec*MenB and Gly-146 of *sc*MenB as part of the active site and is opposite two glycine residues (Gly-86 and Gly-133 in *ec*MenB) whose backbone amides form an oxyanion hole for activation of the substrate and stabilization of the enolate oxyanion intermediate in the MenB-catalyzed intramolecular Claisen condensation. Structural comparison shows that this anion takes the same position and orientation as those in the active sites of *sc*MenB and the *S. typhimurium* MenB (*st*MenB, PDB entry 3H02) and is found to occupy a position equivalent to that of the side chain carboxylate of the essential Asp-185 of *mt*MenB (Figure 3).

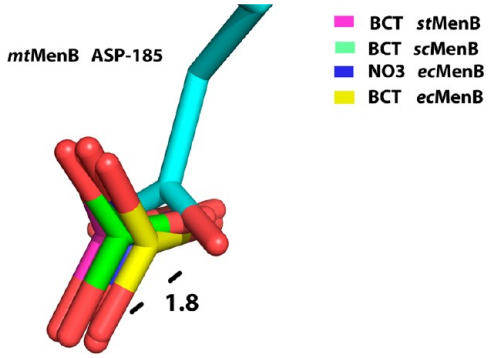

Figure 3. Superposition of the bicarbonate cofactors or nitrate in type I DHNA-CoA synthases and the side chain carboxylate of Asp-185 in the type II *mt*MenB. The bicarbonate (BCT) ions are from the *ec*MenB−HCO_3^- complex, *st*MenB (PDB entry 3H02), and the *sc*MenB−HCO_3^- complex; the nitrate ion is from the *ec*MenB−NO_3^- complex, and the aspartate side chain with cyan carbon atoms is from *mt*MenB in complex with acetoacetyl-CoA (PDB entry 1Q51). The crystal structures are superimposed with PyMol, and only the anions and the side chain of Asp-185 are shown. The number indicates the distance between the two ends of the black dashed line in angstroms.

When the *ec*MenB crystal was grown in the absence of the externally added $NaHCO_3$, no bicarbonate was found in the structure. Instead, a chloride ion was readily identified at the equivalent position, consistent with the finding of a previous study (Figure 2D).[30] However, the structure of the *sc*MenB crystal grown in the absence of externally added $NaHCO_3$ was found to be identical to that of the crystals grown in the presence of 5 mM $NaHCO_3$ and to bind a bicarbonate ion at the same position. This unexpected result effectively validated the finding of a bicarbonate ion in the structure of the *st*MenB crystal grown in the absence of externally added $NaHCO_3$. This is consistent with the high affinity of *sc*MenB for bicarbonate in an activity characterization.[21] Despite the similar bicarbonate affinities of *ec*MenB and *sc*MenB, the absence of bicarbonate ion in the structure of the *ec*MenB crystals grown under similar conditions may be due to inclusion of >150 mM NaCl in buffers used in the current and previous studies,[30] which was not present in the crystallization buffers for *sc*MenB or *st*MenB. Nonetheless, the ready replacement of the chloride ion with bicarbonate in the presence of 5 mM $NaHCO_3$ strongly suggests that bicarbonate is a cognate ligand and binds to the anion binding site of MenB with a much higher affinity than chloride.

When the *ec*MenB crystal was grown in the presence of 5 mM $NaNO_3$, nitrate ion was readily found in the anion binding site of the resulting structure in a position identical to that of the MenB-bound bicarbonate (Figure 3). This finding is highly consistent with the previous kinetic results demonstrating that nitrate inhibits the DHNA-CoA synthase activity of *ec*MenB through competitive inhibition against the bicarbonate binding.[20] The binding of nitrate and bicarbonate to the same anion binding site strongly suggests that bicarbonate binds to the active site and exerts its critical role in the catalytic mechanism of the enzyme.

Factors Contributing to Bicarbonate Binding. In the *ec*MenB−HCO_3^- complex, the bicarbonate anion is within hydrogen bonding distance of the side chain amide of a

dx.doi.org/10.1021/bi300486j | *Biochemistry* 2012, 51, 4580−4589

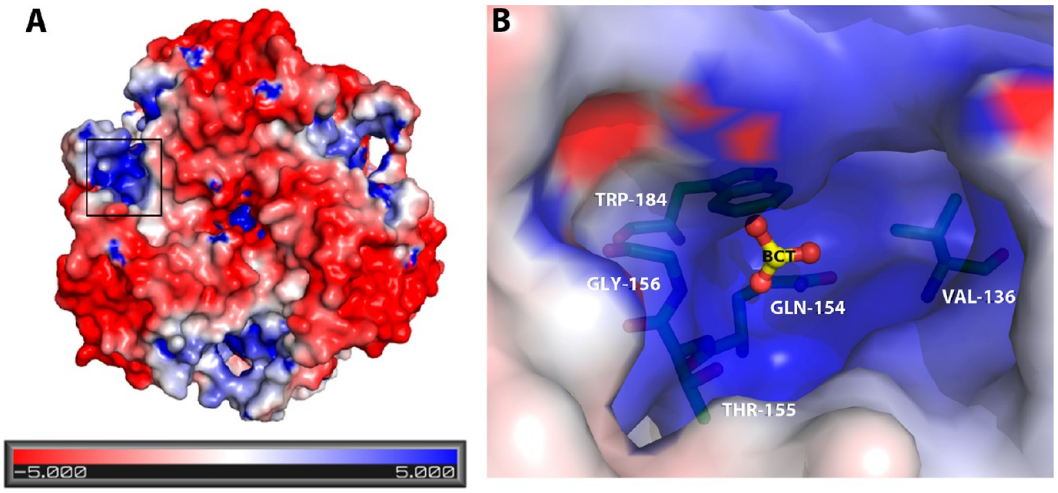

Figure 4. Electrostatic potential surface of the *ec*MenB hexamer viewed through the 3-fold axis of the trimers (A) and the bicarbonate binding site (B) in the *ec*MenB−HCO_3^- complex. The black square in panel A denotes a region corresponding to the enzyme active site. Electrostatic potentials of less than −5 kT, neutral, and greater than 5 kT are colored red, white, and blue, respectively. The bound bicarbonate (BCT) is shown as sticks with a yellow carbon atom, and its surrounding amino acid residues are shown as blue sticks in panel B.

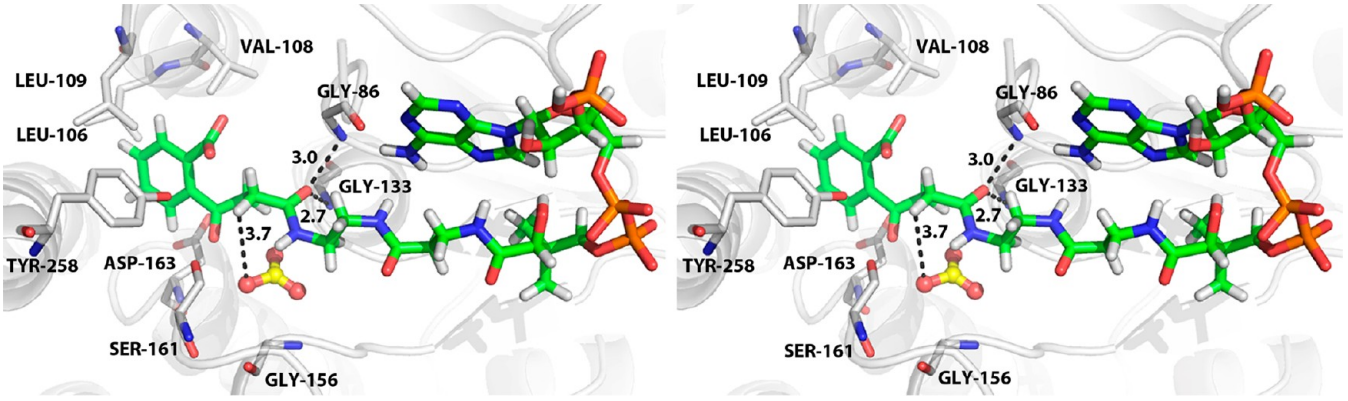

Figure 5. Stereoview of the substrate analogue OSB-NCoA from an enzyme complex (PDB entry 3T88) superimposed into the active site of the *ec*MenB−HCO_3^- complex. The substrate analogue is represented as sticks with H, C, N, P, and O atoms colored white, green, blue, brown, and red, respectively. The conserved active site residues in *ec*MenB are shown as sticks with gray carbons. The hydrogen bonds in the oxyanion hole and the shortest distance between bicarbonate and the pro-*R* α-proton of the substrate analogue are indicated by dashed lines with distances in angstroms.

glutamine (Gln-154) and the backbone amides of Thr-155 and Gly-156 (Figure 2C). The planar anion is tightly packed against the hydrophobic indole ring of the Trp-184 side chain, leaving an unliganded oxygen atom of the exogenous bicarbonate pointing toward the empty active site cavity. The side chain of a valine (Val-136) makes hydrophobic interactions with Trp-184 and may also contribute significantly to binding of the anionic cofactor. In the *sc*MenB−HCO_3^- complex, the coordination environment of the bicarbonate anion is almost the same and the corresponding amino acid residues involved in the binding are Gln-144, Thr-145, Trp-174, and Val-126. These bicarbonate-binding residues are conserved among all other type I MenB orthologues, which contain a conserved glycine residue corresponding to Gly-156 of *ec*MenB.[20] The roles of these residues in bicarbonate binding revealed by the protein structures are strongly supported by the previous kinetic results that the bicarbonate binding affinity is decreased by >20-fold with a concomitant decrease in the DHNA-CoA synthase activity by mutation of Gln-154 or Trp-184 to alanine or phenylalanine, respectively, in *ec*MenB.[20]

Besides the specific interactions, the surface electrostatic potential of the protein was also explored for its potential role in the binding of the small anions. As shown in Figure 4A, a large proportion of the hexameric surface of *ec*MenB exhibits negative electrostatic potential, whereas small isolated regions corresponding to the enzyme active sites near the subunit interface present positive surface electrostatic potential. This unique distribution of electrostatic potential may facilitate capture of the negatively charged OSB-CoA substrate by the enzyme from the bulk solution. Within the active site cavity, the anion binding pocket is covered by a surface with highly positive electrostatic potential (Figure 4B), which is believed to be involved in the capture of the bicarbonate cofactor through nonspecific electrostatic attraction. However, the contribution of this nonspecific electrostatic interaction to the binding of bicarbonate, relative to the specific hydrophobic and hydrogen bonding interactions, is difficult to measure. Nonetheless, the fact that this nonspecific electrostatic attractive force is able to fix a chloride ion without the help of any specific hydrogen bonding interactions in apo-*ec*MenB (Figure 2D) is a clear indication that it also plays a critical role in bicarbonate binding. The positive electrostatic surface of the bicarbonate binding site is partly due to Lys-158, which is opposite Gly-156 in the same helix (H5 in Figure 2B) and conserved among all type I MenB

dx.doi.org/10.1021/bi300486j | *Biochemistry* 2012, 51, 4580−4589

orthologues. It is thus a general feature of all type I MenB proteins, which has genetically evolved as an integral part of the mechanism for binding of the catalytically essential bicarbonate cofactor.

Catalytic Role of the Bicarbonate Ion. To reassess the potential role of the bicarbonate ion in MenB catalysis, the stable analogue *o*-succinylbenzoyl-aminoCoA (OSB-NCoA) of the *o*-succinylbenzoyl-CoA (OSB-CoA) substrate was manually docked into the active site of the *ec*MenB–HCO_3^- complex through superposition with the recently determined crystal structure of the *E. coli* MenB in complex with OSB-NCoA (PDB entry 3T88).[30] Except for an ordered loop containing residues 87–106 in the *ec*MenB complex structure, these two structures extensively overlap and contain most of the identified active site residues in exactly the same position and orientation. After the structures had been superimposed, the polypeptide chain of the MenB–OSB-NCoA complex was removed to leave the substrate analogue in the active site of the *ec*MenB–HCO_3^- complex. As shown in Figure 5, the bicarbonate ion is close to the α-carbon of the substrate analogue in the model, taking a position suitable for abstraction of the pro-*R* α-proton with an estimated distance of 3.7 Å. This analysis suggests that the bicarbonate ion could serve as the essential catalytic base in the MenB-catalyzed reaction, as proposed previously.[20]

The proposed role of the bound bicarbonate cofactor as a catalytic base is consistent with the experimental finding that bicarbonate is essential to the activities of MenB orthologues (type I enzymes) with a conserved glycine residue corresponding to Gly-156 of *ec*MenB.[20,21] It also offers a unified catalytic mechanism for all MenB enzymes in which an equivalent acidic group, either the bound bicarbonate in type I MenB enzymes or the side chain carboxylate of a conserved aspartate with a spatial position equivalent to that of Asp-185 of *mt*MenB in the bicarbonate-independent MenB orthologues (type II enzymes), serves as the essential base for the generation of the enolate intermediate for intramolecular Claisen condensation in the synthesis of DHNA-CoA. This proposal that a conserved acidic group acts as a catalytic base is supported by the presence of an equivalent functional group in other members of the crotonase superfamily. Structurally, the conserved MenB base is equivalent to Glu-164 of enoyl-CoA hydratase (crotonase or ECH),[23,24] Glu-165 of rat mitochondrial enoyl-CoA isomerase (MCI),[53,54] Glu-196 of the rate dienoyl-CoA isomerase (DCI),[55] and Glu-143 of hydroxycinnamoyl-CoA hydratase-lyase (HCHL),[56] which all serve as the catalytic base responsible for the abstraction of a proton from the α-carbon of the coenzyme A thioester. Sequence analysis also shows that an acidic functional group corresponding to Asp-185 of *mt*MenB is conserved among most members of the crotonase superfamily (Figure 6).

The proposed role of the bound bicarbonate cofactor in type I MenB enzymes and the conserved aspartate in type II MenB enzymes is also supported by the experimental finding that the pro-*R* α-proton of the OSB-CoA substrate is abstracted.[31] This pro-*R* stereochemistry is also found in the α-proton abstraction of crotonase[57] and rat liver Δ^3,Δ^5-2,4-dienoyl-CoA isomerase (DCI).[58,59] Moreover, analysis of the topological arrangement of the catalytic base and the bound substrate analogues in crystal structures of other crotonase fold proteins, such as rat mitochondrial 3-enoyl-CoA isomerase[54] and the dioxygenase DpgC,[60,61] also supports pro-*R* specific α-proton abstraction. Thus, despite the finding of pro-2*S* stereochemistry for the reverse Dickmann condensation catalyzed by another crotonase

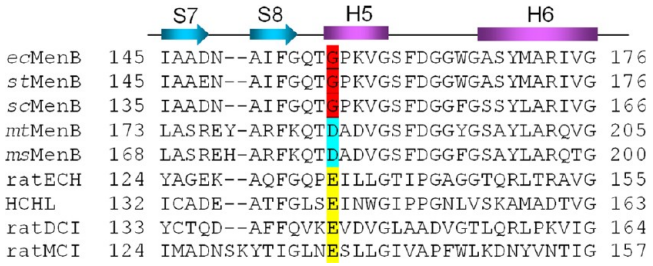

Figure 6. Conservation of a general base among MenBs and other crotonase fold enzymes. The bases in the type I MenBs are bicarbonate ions bound at a position above the underlined conserved glycine residue as found in crystal structures: Gly-156 of *ec*MenB (GI 16130197), Gly-156 of *st*MenB (GI 16761233), and Gly-146 of *sc*MenB (GI 16330127). The bases in type II *mt*MenB (GI 15607688) and *ms*MenB (GI 118472778) are Asp-185 and Asp-180, respectively. A conserved glutamate residue has been experimentally shown to be the catalytic base responsible for the abstraction of a proton from the α-carbon of the thioester substrates in other crotonase fold enzymes, including Glu-164 of rate crotonase (ratECH, GI 3212678), Glu-165 of rat mitochondrial enoyl-CoA isomerase (ratMCI, GI 56967286), Glu-196 of the rate dienoyl-CoA isomerase (ratDCI, GI 4699607), and Glu-143 of hydroxycinnamoyl-CoA hydratase-lyase (HCHL, GI 189096078). The sequences were aligned with ClustalW, and the residues corresponding to the conserved base are highlighted in red for type I MenBs, blue for type II MenBs, and green for other crotonase superfamily members. The secondary structures above the sequences are from *ec*MenB illustrated in Figure 2B, which are represented as arrows for β-pleated sheets and rectangles for α-helices.

fold enzyme BadI,[62] which is consistent with the alternate catalytic mechanism for MenB,[29,30] the proposed role of the conserved acidic group in MenB enzymes unifies the catalytic mechanism of many members of the crotonase superfamily in that a conserved catalytic base and a conserved pro-*R* stereochemistry are involved in the α-proton abstraction.

Except for the conserved acidic group corresponding to the bicarbonate cofactor in type I MenB enzymes and Asp-185 of *mt*MenB in type II enzymes, there is another catalytically essential acidic aspartic acid residue corresponding to Asp-163 of *ec*MenB[63] or Asp-192 of *mt*MenB,[29] which is strictly conserved among all MenB enzymes.[20] These two conserved acidic groups are reminiscent of the two active site glutamic acids in crotonase, Glu-144 and Glu-164 that are crucial to enzyme activity. In crotonase catalysis, Glu-144 is connected to the catalytic base Glu-164 by an active site water molecule through hydrogen bonding and acts in concert with the latter to effect *syn* addition of a water molecule to a 2-enoyl-CoA substrate or *syn* elimination of a water molecule from a 3-hydroxyalkanoyl-CoA substrate in either an E1cb or a concerted mechanism.[64,65] Currently, it is not known whether the second conserved aspartate in MenB would resemble Glu-144 of crotonase to interact with the catalytic base in the catalytic mechanism. Although it is suggested to participate in catalysis after ligand-induced conformational change,[63] this second conserved base is separated from the catalytic base by >5.1 Å and is not posed suitably for catalysis in the known crystal structures of *mt*MenB or the holo form of *ec*MenB, *sc*MenB, or *st*MenB. Further investigation is needed to probe the role of this second conserved acidic group in the MenB catalytic mechanism.

Summary. In this study, we determined the crystal structures of the MenB orthologues from *E. coli* (*ec*MenB) and *Synechocystis* sp. PCC6803 (*sc*MenB) in the presence and

dx.doi.org/10.1021/bi300486j | *Biochemistry* 2012, 51, 4580–4589

absence of externally added bicarbonate. In the meantime, we have also determined the crystal structure of *ec*MenB in complex with nitrate, an inhibitor directly competing with bicarbonate.[20] These crystal structures unequivocally demonstrate that bicarbonate is bound to the active site at a position corresponding to Gly-156 of *ec*MenB, which is strictly conserved among all type I MenB enzymes. In addition, the crystallographic results also show that the type I MenB enzymes are indeed able to trap bicarbonate in their active sites in open air even without externally added bicarbonate in the buffer, thus validating the previous finding of a bicarbonate ion in the active site of the enzyme from *S. typhimurium* (*st*MenB). This finding of bicarbonate at the MenB active site provides a solid structural basis for the dependence of DHNA-CoA synthase activity of type I enzymes on the simple anion. The location of the bicarbonate ion in relation to a modeled substrate analogue at the enzyme active sites strongly supports the idea that the anionic cofactor serves as the catalytic base in abstraction of a proton from the α-carbon of the coenzyme A thioester substrate.

AUTHOR INFORMATION

Corresponding Author

*Z.G.: Department of Chemistry, The Hong Kong University of Science and Technology, Clear Water Bay, Kowloon, Hong Kong SAR, China; telephone, 852-2358-7352; fax, 852-2358-1594; e-mail, chguo@ust.hk. J.Z.: Shanghai Institute of Organic Chemistry, Chinese Academy of Sciences, 345 Lingling Rd., Shanghai 200032, China; telephone, 86-21-54925377; fax, 86-21-64166128; e-mail, jiahai@mail.sioc.ac.cn.

Present Addresses

[§]Department of Chemical and Biological Engineering, State University of New York at Buffalo, Buffalo, NY 14260.
[∥]Life Sciences Institute, University of Michigan, Ann Arbor, MI 48109-2216.

Funding

This work was supported by Grants GRF601209 and RPC11SC16 from the Research Grants Council of the Government of the Hong Kong Special Administrative Region (to Z.G.) and Grant 2009CB918600 from the National Program on Key Basic Research of China (to J.Z.).

Notes

The authors declare no competing financial interest.

ACKNOWLEDGMENTS

We thank S. Huang and J. He at the BL17U beamline of the Shanghai Synchrotron Radiation Facility (SSRF) for assistance with data collection. We also thank Prof. Zong-Xiang Xia for critically reading the manuscript.

ABBREVIATIONS

CoA, coenzyme A; DHNA-CoA, 1,4-dihydroxy-2-naphthoyl-CoA; SHCHC, (1*R*,6*R*)-2-succinyl-6-hydroxy-2,4-cyclohexadiene-1-carboxylate; OSB-CoA, *o*-succinylbenzoyl-CoA; IPTG, isopropyl β-D-thiogalactopyranoside; *ec*MenB, *sc*MenB, *mt*MenB, *st*MenB, *sa*MenB, and *gk*MenB, MenB orthologues from *E. coli*, *Synechocystis* sp. PCC6803, *M. tuberculosis*, *S. typhimurium*, *St. aureus*, and *G. kaustophilus* HTA 426, respectively.

REFERENCES

(1) Meganathan, R. (2001) Biosynthesis of menaquinone (Vitamin K2) and ubiquinone (Coenzyme Q): A perspective on enzymatic mechanisms. *Vitam. Horm. 61*, 173−218.

(2) Gross, J., Meurer, J., and Bhattacharya, D. (2008) Evidence of a chimeric genome in the cyannobacterial ancestor of plastids. *BMC Evol. Biol. 8*, 117.

(3) Shem, A. B., Frolow, F., and Nelson, N. (2003) Crystal structure of plant photosystem I. *Nature 426*, 630−635.

(4) Jiang, M., Cao, Y., Guo, Z.-F., Chen, M., Chen, X., and Guo, Z. (2007) Menaquinone biosynthesis in *Escherichia coli*: Identification of 2-succinyl-5-enolpyruvyl-6-hydroxyl-3- cyclohexene-1-carboxylate (SEPHCHC) as a novel intermediate and re-evaluation of MenD activity. *Biochemistry 46*, 10979−10989.

(5) Jiang, M., Chen, M., Cao, Y., Yang, Y., Sze, K. H., Chen, X., and Guo, Z. (2007) Determination of the stereochemistry of 2-succinyl-5-enolpyruvyl-6-hydroxy-3-cyclohexene-1-carboxylic acid, a key intermediate in menaquinone biosynthesis. *Org. Lett. 9*, 4765−4767.

(6) Jiang, M., Chen, X., Guo, Z.-F., Cao, Y., Chen, M., and Guo, Z. (2008) Identification and characterization of (1*R*,6*R*)-2-succinyl-6-hydroxy-2,4-cyclohexadiene-1-carboxylate synthase in the menaquinone biosynthesis of *Escherichia coli*. *Biochemistry 47*, 3426−3434.

(7) Berkner, K. L. (2005) The vitamin K-dependent carboxylase. *Annu. Rev. Nutr. 25*, 127−149.

(8) Kurosu, M., Narayanasamy, P., Biswas, K., Dhiman, R., and Crick, D. C. (2007) Discovery of 1,4-dihydroxy-2-naphthoate prenyltransferase inhibitors: New drug leads for multidrug-resistant Gram-positive pathogens. *J. Med. Chem. 50*, 3973−3975.

(9) Lu, X., Zhang, H., Tonge, P. J., and Tan., D. S. (2008) Mechanism-based inhibitors of MenE, an acyl-CoA synthetase involved in bacterial menaquinone biosynthesis. *Bioorg. Med. Chem. Lett. 18*, 5963−5966.

(10) Fang, M., Toogood, R. D., Macova, A., Ho, K., Franzblau, S. G., McNeil, M. R., Sanders, D. A. R., and Palmer, D. R. J. (2010) Succinylphosphonate esters are competitive inhibitors of MenD that show active-site discrimination between homologous α-ketoglutarate-decarboxylating enzymes. *Biochemistry 49*, 2672−2679.

(11) Li, X., Liu, N., Zhang, H., Knudson, S. E., Slayden, R. A., and Tonge, P. J. (2010) Synthesis and SAR studies of 1,4-benzoxazine MenB inhibitors: Novel antibacterial agents against *Mycobacterium tuberculosis*. *Bioorg. Med. Chem. Lett. 20*, 6306−6309.

(12) Li, X., Liu, N., Zhang, H., Knudson, S. E., Li, H. J., Lai, C. T., Simmerling, C., Slayden, R. A., and Tonge, P. J. (2011) CoA adducts of 4-oxo-4-phenylbut-2-enoates: Inhibitors of MenB from the *M. tuberculosis* menaquinone biosynthesis pathway. *ACS Med. Chem. Lett. 2*, 818−823.

(13) Lu, X., Zhou, R., Sharma, I., Li, X., Kumar, G., Swaminathan, S., Tonge, P. J., and Tan, D. S. (2012) Stable analogues of OSB-AMP: Potent inhibitors of MenE, the *o*-succinylbenzoate-CoA synthetase from bacterial menaquinone biosynthesis. *ChemBioChem 13*, 129−136.

(14) Sharma, V., Suvarna, K., Meganathan, R., and Hudspeth, M. E. S. (1992) Menaquinone (Vitamin K2) biosynthesis: Nucleotide sequence and expression of the menB gene from *Escherichia coli*. *J. Bacteriol. 174*, 5057−5062.

(15) Forsyth, R. A., Haselbeck, R. J., Ohlsen, K. L., Yamamoto, R. T., Xu, H., Trawick, J. D., Wall, D., Wang, L., Vickie, B. D., Froelich, J. M., Kedar, G. C., King, P., McCarthy, M., Malone, C., Misiner, B., Robbins, D., Tan, Z., Zhu, Z., Carr, G., Mosca, D. A., Zamudio, C., Foulkes, J. G., and Zyskind, J. W. (2002) A genome-wide strategy for the identification of essential genes in *Staphylococcus aureus*. *Mol. Microbiol. 43*, 1387−1400.

(16) Kobayashi, K., Ehrlich, S. D., Albertini, A., Amati, G., Andersen, K. K., Arnaud, M., Asai, K., Ashikaga, S., Aymerich, S., Bessieres, P., Boland, F., Brignell, S. C., Bron, S., Bunai, K., Chapuis, J., Christiansen, L. C., Danchin, A., Débarbouille, M., Dervyn, E., Deuerlin, E., Devine, K., Devine, S. K., Dreesen, O., Errington, J., Fillinger, S., Foster, S. J., Fujita, Y., Galizzi, A., Gardan, R., Eschevins, C., Fukushima, T., Haga, K., Harwood, C. R., Hecker, M., Hosoya, D., Hullo, M. F., Kakeshita, H., Karamata, D., Kasahara, Y., Kawamura, F., Koga, K., Koski, P.,

Kuwana, R., Imamura, D., Ishimaru, M., Ishikawa, S., Ishio, I., LeCoq, D., Masson, A., Mauël, C., Meima, R., Mellado, R. P., Moir, A., Moriya, S., Nagakawa, E., Nanamiya, H., Nakai, S., Nygaard, P., Ogura, M., Ohanan, T., O'Reilly, M., O'Rourke, M., Pragai, Z., Pooley, H. M., Rapoport, G., Rawlins, J. P., Rivas, L. A., Rivolta, C., Sadaie, A., Sadaie, Y., Sarvas, M., Sato, T., Saxild, H. H., Scanlan, E., Schumann, W., Seegers, J. F., Sekiguchi, J., Sekowska, A., Séror, S. J., Simon, M., Stragier, P., Studer, R., Takamatsu, H., Tanaka, T., Takeuchi, M., Thomaides, H. B., Vagner, V., vanDijl, J. M., Watabe, K., Wipat, A., Yamamoto, H., Yamamoto, M., Yamamoto, Y., Yamane, K., Yata, K., Yoshida, K., Yoshikawa, H., Zuber, U., and Ogasawara, N. (2003) Essential *Bacillus subtilis* genes. *Proc. Natl. Acad. Sci. U.S.A. 100*, 4678−4683.

(17) Akerley, B. J., Rubin, E. J., Novick, V. L., Amaya, K., Judson, N., and Mekalanos, J. J. (2002) A genome-scale analysis for identification of genes required for growth or survival of *Haemophilus influenzae*. *Proc. Natl. Acad. Sci. U.S.A. 99*, 966−971.

(18) Johnson, T. W., Shen, G., Zybailov, B., Kolling, D., Reategui, R., Beauparlant, S., Vassiliev, I. R., Bryant, D. A., Jones, A. D., Golbeck, J. H., and Chitnis, P. R. (2000) Recruitment of a foreign quinone into the A1 site of photosystem I I. Genetic and physiological characterization of phylloquinone biosynthetic pathway mutants in *Synechocystis* sp. PCC 6803. *J. Biol. Chem. 275*, 8523−8530.

(19) Gross, J., Cho, W. K., Lezhneva, L., Falk, J., Krupinska, K., Shinozaki, K., Seki, M., Herrmann, R. G., and Meurer, J. (2006) A plant locus essential for phylloquinone (Vitamin K1) biosynthesis originated from a fusion of four eubacterial genes. *J. Biol. Chem. 281*, 17189−17196.

(20) Jiang, M., Chen, M., Guo, Z. F., and Guo, Z. (2010) A bicarbonate cofactor modulates 1,4-dihydroxy-2-naphthoyl coenzyme A synthase in menaquinone biosynthesis of *Escherichia coli*. *J. Biol. Chem. 285*, 30159−30169.

(21) Song, H., and Guo, Z. (2012) Characterization of 1,4-dihydroxy-2-naphthoyl-coenzyme A synthase (MenB) in phylloquinone biosynthesis of *Synechocystis* sp. PCC 6803. *Sci. China, Ser. B: Chem. 55*, 98−105.

(22) D'Ordine, R. L., Bahnson, B. J., Tonge, P. J., and Anderson, V. E. (1994) Enoyl-coenzyme A hydratase-catalyzed exchange of the α-protons of coenzyme A thiol esters: A model for an enolized intermediate in the enzyme-catalyzed elimination. *Biochemistry 33*, 14733−14742.

(23) Newen, G. M., Janssen, U., and Stoffel, W. (1995) Enoyl-CoA hydratase and isomerase form a superfamily with a common active-site glutamate residue. *Eur. J. Biochem. 228*, 68−73.

(24) Engel, C. K., Mathieu, M., Zeelen, J. P., Hiltunen, J. K., and Wierenga, R. K. (1996) Crystal structure of enoyl-coenzyme A (CoA) hydratase at 2.5 Å resolution: A spiral fold defines the CoA-binding pocket. *EMBO J. 19*, 5135−5145.

(25) Engel, C. K., Kiema, T. R., Hiltunen, J. K., and Wierenga, R. K. (1998) The crystal structure of enoyl-CoA hydratase complexed with octanoyl-CoA reveals the structural adaptations required for binding of a long chain fatty acid-CoA molecule. *J. Mol. Biol. 275*, 847−859.

(26) Modis, Y., Filppula, S. A., Novikov, D. K., Norledge, B., Hiltunen, J. K., and Wierenga, R. K. (1998) The crystal structure of dienoyl-CoA isomerase at 1.5 Å resolution reveals the importance of aspartate and glutamate side chains for catalysis. *Structure 6*, 957−970.

(27) Kiema, T. R., Engel, C. K., Schmitz, W., Filppula, S. A., Wierenga, R. K., and Hiltunen., J. K. (1999) Mutagenic and enzymological studies of the hydratase and isomerase activities of 2-enoyl-CoA hydratase-1. *Biochemistry 38*, 2991−2999.

(28) Mursula, A. M., van Aalten, D. M. F., Hiltunen, J. K., and Wierenga, R. K. (2001) The crystal structure of Δ^3-Δ^2-enoyl-CoA isomerase. *J. Mol. Biol. 309*, 845−853.

(29) Truglio, J. J., Theis, K., Feng, Y., Gajda, R., Machutta, C., Tonge, P. J., and Kisker, C. (2003) Crystal structure of *Mycobacterium tuberculosis* MenB, a key enzyme in vitamin K_2 biosynthesis. *J. Biol. Chem. 278*, 42352−42360.

(30) Li, H. L., Li, X., Liu, N., Zhang, H., Truglio, J. J., Mishra, S., Kisker, C. F., Garcia-Diaz, M., and Tonge, P. J. (2011) Mechanism of the intramolecular Claisen condensation reaction catalyzed by MenB, a crotonase superfamily member. *Biochemistry 50*, 9532−9544.

(31) Igbavboa, U., and Leistner, E. (1990) Sequence of function in the crotonase superfamily: The stereochemistry course of the reaction catalyzed by naphthoate synthase, an enzyme involved in menaquinone (vitamin K2) biosynthesis. *Eur. J. Biochem. 192*, 441−449.

(32) Minasov, G., Wawrzak, Z., Skarina, T., Onopriyenko, O., Peterson, S. N., Savchenko, A., and Anderson, W. F. (2009) 2.15 Angstrom resolution crystal structure of naphthoate synthase from *Salmonella typhimurium*. Center for Structural Genomics of Infectious Diseases, DOI: 10.2210/pdb3h02/pdb.

(33) Ulaganathan, V., Agacan, M. F., Buetow, L., Tulloch, L. B., and Hunter, W. N. (2007) Structure of *Staphylococcus aureus* 1,4-dihydroxy-2-naphthoyl-CoA synthase (MenB) in complex with acetoacetyl-CoA. *Acta Crystallogr. F63*, 908−913.

(34) Kanaujia, S. P., Ranjani, C. V., Jeyakanthan, J., Baba, S., Kuroishi, C., Ebihara, A., Shinkai, A., Kuramitsu, S., Shiro, Y., Sekar, K., and Yokoyama, S. (2007) Cloning, expression, purification, crystallization and preliminary X-ray crystallographic study of DHNA synthetase from *Geobacillus kaustophilus*. *Acta Crystallogr. F63*, 103−105.

(35) Jiang, M., and Guo, Z. (2007) Effects of macromolecular crowding on the intrinsic catalytic efficiency and structure of enterobactin-specific isochorismate synthase. *J. Am. Chem. Soc. 129*, 730−731.

(36) Jiang, M., Chen, X., Wu, X. H., Chen, M., Wu, Y., and Guo, Z. (2009) Catalytic mechanism of SHCHC synthase in the menaquinone biosynthesis of *Escherichia coli*: Identification and mutational analysis of the active site residues. *Biochemistry 48*, 6921−6931.

(37) Grisostomi, G., Kast, P., Pulido, R., Huynh, J., and Hilvert, D. (1997) Efficient in vivo synthesis and rapid purification of chorismic acid using an engineered *Escherichia coli* strain. *Bioorg. Chem. 25*, 297−305.

(38) Otwinowski, Z., and Minor, W. (1997) Processing of X-ray diffraction data collected in oscillation mode. *Methods Enzymol. 276*, 307−326.

(39) Battye, T. G. G., Kontogiannis, L., Johnson, O., Powell, H. R., and Leslie, A. G. W. (2011) iMOSFLM: A new graphical interface for diffraction-image processing with MOSFLM. *Acta Crystallogr. D67*, 271−281.

(40) Collaborative Computational Project, Number 4 (1994) The CCP4 Suite: Programs for Protein Crystallography. *Acta Crystallogr. D50*, 760−763.

(41) McCoy, A. J., Grosse-Kunstleve, R. W., Adams, P. D., Winn, M. D., Storoni, L. C., and Read, R. J. (2007) Phaser crystallographic software. *J. Appl. Crystallogr. 40*, 658−674.

(42) Emsley, P., Lohkamp, B., Scott, W. G., and Cowtan, K. (2010) Features and development of *Coot*. *Acta Crystallogr. D66*, 486−501.

(43) Adams, P. D., Afonine, P. V., Bunkoczi, G., Chen, V. B., Davis, I. W., Echols, N., Headd, J. J., Hung, L. W., Kapral, G. J., Grosse-Kunstleve, R. W., McCoy, A. J., Moriarty, N. W., Oeffner, R., Read, R. J., Richardson, D. C., Richardson, J. S., Terwilliger, T. C., and Zwart, P. H. (2010) PHENIX: A comprehensive Python-based system for macromolecular structure solution. *Acta Crystallogr. D66*, 213−221.

(44) Vagin, A. A., Steiner, R. S., Lebedev, A. A., Potterton, L., McNicholas, S., Long, F., and Murshudov, G. N. (2004) REFMAC5 dictionary: Organisation of prior chemical knowledge and guidelines for its use. *Acta Crystallogr. D60*, 2284−2295.

(45) Moriarty, N. W., Grosse-Kunstleve, R. W., and Adams, P. D. (2009) electronic Ligand Builder and Optimization Workbench (eLBOW): A tool for ligand coordinate and restraint generation. *Acta Crystallogr. D65*, 1074−1080.

(46) Chen, V. B., Arendall, W. B., Headd, J. J., Keedy, D. A., Immormino, R. M., Kapral, G. J., Murray, L. W., Richardson, J. S., and Richardson, D. C. (2010) MolProbity: All-atom structure validation for macromolecular crystallography. *Acta Crystallogr. D66*, 12−21.

(47) Laskowski, R. A., MacArthur, M. W., Moss, D. S., and Thornton, J. M. (1993) PROCHECK: A program to check the stereochemical quality of protein structures. *J. Appl. Crystallogr. 26*, 283−291.

(48) DeLano, W. L. (2002) *The PyMOL Molecular Graphics System*, DeLano Scientific, San Carlos, CA.
(49) Baker, N. A., Sept, D., Joseph, S., Holst, M. J., and McCammon, J. A. (2001) Electrostatics of nanosystems: Application to microtubules and the ribosome. *Proc. Natl. Acad. Sci. U.S.A. 98*, 10037−10041.
(50) Dolinsky, T. J., Nielsen, J. E., McCammon, J. A., and Baker, N. A. (2004) PDB2PQR: An automated pipeline for the setup, execution, and analysis of Poisson-Boltzmann electrostatics calculations. *Nucleic Acids Res. 32*, W665−W667.
(51) Larkin, M. A., Blackshields, G., Brown, N. P., Chenna, R., McGettigan, P. A., McWilliam, H., Valentin, F., Wallace, I. M., Wilm, A., Lopez, R., Thompson, J. D., Gibson, T. J., and Higgins, D. G. (2007) Clustal W and Clustal X version 2.0. *Bioinformatics 23*, 2947−2948.
(52) Johnston, J. M., Arcus, V. L., and Baker, E. N. (2005) Structure of naphthoate synthase (MenB) from *Mycobacterium tuberculosis* in both native and product-bound forms. *Acta Crystallogr. D61*, 1199−1206.
(53) Muller-Newen, G., and Stoffel, W. (1993) Site-directed mutagenesis of putative active-site amino acid residues of 3,2-transenoyl-CoA isomerase, conserved within the low-homology isomerase/hydratase enzyme family. *Biochemistry 32*, 11405−11412.
(54) Hubbard, P. A., Yu, W., Schulz, H., and Kim, J. J. P. (2005) Domain swapping in the low-similarity isomerase/hydratase superfamily: The crystal structure of rat mitochondrial Δ^3,Δ^2-enoyl-CoA isomerase. *Protein Sci. 14*, 1545−1555.
(55) Modis, Y., Filppula, S. A., Novikov, D. K., Norledge, B., Hiltunen, J. K., and Wierenga, R. K. (1998) The crystal structure of dienoyl-CoA isomerase at 1.5 Å resolution reveals the importance of aspartate and glutamate sidechains for catalysis. *Structure 6*, 957−970.
(56) Bennett, J. P., Bertin, L., Moulton, B., Fairlamb, I. J. S., Brzozowski, A. M., Walton, N. J., and Grogan, G. (2008) A ternary complex of hydroxycinnamoyl-CoA hydratase-lyase (HCHL) with acetyl-CoA and vanillin gives insights into substrate specificity and mechanism. *Biochem. J. 414*, 281−289.
(57) Willadsen, P., and Eggerer, H. (1975) Substrate stereochemistry of the acetyl-CoA acetyltransferase reaction. *Eur. J. Biochem. 54*, 253−258.
(58) Chen, L. S., Jin, S. J., and Tserng, K. Y. (1994) Purification and mechanism of Δ^3,Δ^5-*t*-2,*t*-4-dienoyl-CoA isomerase from rat liver. *Biochemistry 33*, 10527−10534.
(59) Fillgrove, K. L., and Anderson, V. E. (2000) Orientation of coenzyme A substrates, nicotinamide and active site functional groups in (Di)enoylcoenzyme A reductases. *Biochemistry 39*, 7001−7011.
(60) Widboom, P., Fielding, E. N., Liu, Y., and Bruner, S. D. (2007) Structural basis for cofactor-independent dioxygenation in vancomycin biosynthesis. *Nature 447*, 342−345.
(61) Fielding, E. N., Widboom, P. F., and Bruner, S. D. (2007) Substrate recognition and catalysis by the cofactor-independent dioxygenase DpgC. *Biochemistry 46*, 13994−14000.
(62) Eberhard, E. D., and Gerlt, J. A. (2004) Evolution of function in the crotonase superfamily: The stereochemical course of the reaction catalyzed by 2-ketocyclohexanecarboxyl-CoA hydrolase. *J. Am. Chem. Soc. 126*, 7188−7189.
(63) Chen, M., Jiang, M., Sun, Y., Guo, Z. F., and Guo, Z. (2011) Stabilization of the second oxyanion intermediate by 1,4-dihydroxy-2-naphthoyl coenzyme A synthase of the menaquinone pathway: Spectroscopic evidence of the involvement of a conserved aspartic acid. *Biochemistry 50*, 5893−5904.
(64) Hofstein, H. A., Feng, Y., Anderson, V. E., and Tonge, P. J. (1999) Role of glutamate 144 and glutamate 164 in the catalytic mechanism of enoyl-CoA hydratase. *Biochemistry 38*, 9508−9516.
(65) Bahnson, B. J., Anderson, V. E., and Petsko., G. A. (2002) Structural mechanism of enoyl-CoA hydratase: Three atoms from a single water are added in either an E1cb stepwise or concerted fashion. *Biochemistry 41*, 2621−2629.